MULTIAXIALITY QUOTIENT AS FUNCTION OF CRACK DEPTH AND LOAD FOR SELECTED SPECIMEN AND COMPONENT GEOMETRIES

D. UHLMANN and H. DIEM*

The level of multiaxiality of stress state in the ligament of cracked components is of special interest to delineate the failure process of defective components made of ductile materials apart from the level of the parameter J-Integral. Five different geometries, three specimen geometries (CT, CST and SECT) and two pipe geometries with axially and circumferentially oriented cracks were analysed with the help of finite element analyses.The multiaxiality q changes with increasing crack depth as a function of geometry and load. For all geometries and load configurations small q-values are found only in a confined area of the ligament.

INTRODUCTION

Finite-element-analyses of cracked structures enable a statement to be made on the stress relations in the ligament as function of the crack depth ratio and the load. In view of the crack extension of ductile materials it is of special interest whether extreme (triaxial) tensile stress states may cause instable crack extension and failure due to cleavage fracture. This subject is studied worldwide. The level of multiaxiality of stress state seems to be an appropriate parameter to assess the mode of failure behaviour. The international effort on this subject is documented in numerous publications, e.g. (1-5).

The multiaxiality quotient as defined by Clausmeyer (1, 6) $q = \sigma_v/(\sqrt{3}\cdot\bar{\sigma})$ with σ_v = v. Mises stress and $\bar{\sigma} = (\sigma_1+\sigma_2+\sigma_3)/3$, will be used in this paper. According to

*Staatliche Materialprüfungsanstalt (MPA), University of Stuttgart, Pfaffenwaldring 32, D-70569 Stuttgart

this definition small q-values indicate a high multiaxiality of stress state. Investigations on the effect of stress state on failure behaviour of large tensile specimen have been published in (7). The aim of the present paper is to provide further information about initial linear-elastic q-distributions by a large variation of crack depth for three specimen geometries (dominant bending, bending and tension and dominant tension) and two pipe geometries (axial and circuferential cracks). It is necessary to mention that for a detailed assessment in addition to the linear-elastic results which are mainly presented in this paper elastic-plastic solutions are necessary. For selected crack geometries additional elastic-plastic FE-solutions are given.

For the transferability of specimen results to component assessment it is very important to have an information which specimen is adequate to describe the component behaviour. In this paper single-edge precracked specimen and components are taken into consideration against the background of the transferability. Double-edge notched or cracked specimen (DENT, DECT) are known to be of high multiaxility over the whole ligament (8). However, such kind of crack formation is rather improbable in practice.

GEOMETRY AND BOUNDARY CONDITIONS

The CT-, C-shape (CST) and SECT-specimen were selected as geometries for the parametric, numerical study. Figure 1. In the calculations the crack depth ratio was varied between a_i/W = 0.1 and 0.9. In this numerical study no experimental limitations on crack depth for special specimen geometries are taken into account. However it has to be mentioned, that it is not possible to provide reliable experimental data with CT-specimen having low a/W-ratios. In order to have comparable relations like in the component analysis which was simultaneously performed, the specimen width W was assumed in conformity with the wall thickness t of the component (W = t = 28,7 mm). Each of the two-dimensional FE-analyses of the specimen was made on the assumption of plane strain condition.

A pipe cross-section with an inner diameter of 425 mm and the crack position in axial direction was considered as component geometry. On the assumption that there is a plane strain state a variation between a_j/t = 0.1 and 0.9 was made in the calculations. The results for the axial cracks were completed using results from expensive

three-dimensional FE-analyses of inner circumferentially oriented cracks. These analyses were carried out within the scope of the HDR-safety programme (9). In this case the wall thickness was 16 mm. The size of the circumferential cracks was $2\alpha_c = 60°$ and the analysed crack depth ratios were $a_j/t = 0.25$, 0.50 and 0.75.

The load cases internal pressure and bending were investigated for the axial and circumferential cracks. Stressing due to thermal stratification was added as the third load case.

The characterization of the considered ferritic material 20 MnMoNi 5 5 is documented in detail in (10). The material properties at temperature T = 240 °C are: $R_{p0.2}$ = 440 MPa, R_m = 599 MPa and A_5 = 18.9 %. The material is at T = 240 °C with a value of 150 J (TS-direction) in the upper shelf of the notch impact energy.

SPECIMEN RESULTS

The results of the multiaxiality quotient as function of the crack depth ratio in the ligament of a CT-specimen are delineated in Figure 2. The extension of the area of high multiaxiality (q_{min} ~ 0,27 (8)) depends on the crack depth ratio. In the linear-elastic FE-analyses the largest area of high multiaxiality is calculated for the crack depth ratio a_1/W = 0,1. At all other analysed crack depth ratios there is only a local minimum of the q-factor in the ligament followed by an immediate increase.

In order to investigate the change of the multiaxiality quotient during material plastification in comparison to pure elastic behaviour the q-course for the CT-specimen with the crack depth ratio a_5/W = 0.5 was additionally determined with elastic-plastic material behaviour. Figure 2 delineates for the considered material the q-course of a load at a level corresponding to the experimentally determined physical crack initiation value J_i ~ 90 N/mm. The area of high multiaxiality of the CT-specimen with a_5/W = 0.5 increases during elastic-plastic material behaviour in comparison to linear-elastic behaviour. This finding corresponds with the results in (11).

The results of the multiaxiality quotient in the ligament of the C-shaped-specimen are shown in Figure 3. The largest area of high mulitaxiality is for the crack

depth ratio $a_2/W = 0.2$. However, if plastification occurs at the crack tip the multiaxiality will decrease.

The results of the SECT-specimen are delineated in Figure 4. Concerning this specimen geometry the largest area of high multiaxiality ($q_{min} \sim 0.27$) can be found for the crack depth ratio $a_5/W = 0.5$. If this crack depth ratio is analysed considering elastic-plastic material behaviour the area of low q-values decreases analogous to the C-shape-specimen. This means yielding will reduce the multiaxiality.

The results show for each of the three specimen geometries one crack depth ratio with the largest area of high multiaxiality in the ligament. Furthermore, independent on the crack depth ratio, high multiaxiality occurs only in a delimited area of the ligament.

COMPONENT RESULTS

For a pipe cross-section with an axial crack under bending load the results of the q-distribution on the basis of plane strain condition are as shown in Figure 5. These q-distributions correspond well with the results of the C-shaped-specimen. This means, the largest area of high multiaxiality occurs at the crack depth ratio $a_2/t = 0.2$.

Concerning the load case internal pressure, the multiaxiality quotient remains in case of an axial crack with $a_5/t = 0.5$ on a low level for the largest part of the ligament, Figure 6. For any crack depth ratio the q-distributions of the SECT-specimen agree well with those of the pipe cross-section loaded by internal pressure. In case of elastic-plastic material behaviour the multiaxiality in the ligament decreases at $a_5/t = 0.5$ analogous to the behaviour of the SECT-geometry.

The results of the linear-elastic FE-analyses for the circumferential cracks are shown in Figure 7. As mentioned above, only the crack depth ratios $a_j/t = 0.25$, 0.50 and 0.75 were considered. However, the small amount of data is still sufficient for the fact that the multiaxiality quotient concerning the three calculated load cases bending, internal pressure and temperature stratification showed low q-values only in a defined area of the ligament. The q-distributions correspond best with those of the SECT-specimen.

Thus the investigated single-edge precracked specimen and components may be subjected to a classification in view of their q-plot, Figure 8. Independent of the external loading three types will result, a dominating bending load (type 1), a combined bending and tensile load (type 2) and a dominating tensile load (type 3). The crack depth which reveals the largest area of high multiaxiality $(q_{min})_{max}$ can be given for each type. The elastic-plastic FE-analyses show that for the considered material both decrease and increase in the multiaxiality of the ligament is possible as a function of the chosen geometry and crack configuration.

SUMMARY

The linear-elastic and elastic-plastic calculations have shown that for single-edge precracked specimen and component geometries under the load cases bending and tension (or internal pressure) a high multiaxiality is present only in a delimited area of the ligament. Furthermore, there are specimen geometries of which the q-distributions of varying crack depth agree with those of components. Additional investigations in the elastic-plastic regime are required to quantify the reduction in stable crack extension following the attainment of the physical crack initiation value J_i by the multiaxiality in the ligament. An example on the transferability of specimen results to component assessment taking into account the comparability of the multiaxiality of stress state in the ligament is represented in (12).

REFERENCES

(1) Clausmeyer, H. "Über die Beanspruchung von Stahl bei mehrachsigen Spannungszuständen". Konstruktion 20 (1968), Heft 10, S. 395-401

(2) Shih, .F., O'Dowd, N.P. and Kirk, M.T. A Framework for Quantifying Crack Tip Constraint. ASTM Symposium on Constraint Effects in Fracture, May 8-9, 1991, Indianapolis, Indiana, USA

(3) Hancock, J.W., Reuter, W.G. and Parks, D.M. Constraint and Toughness Parameterised by T. ASTM Symposium on Constraint and Fracture, May 8-9, 1991, Indianapolis, Indiana, USA

(4) Brocks, W., Schmitt, W. The Role of Crack Tip Constraint for Ductile Tearing. ECF 8, Turin 1990, Vol. II, S. 1023-1032

(5) Aurich, D., Sommer, E. The Effect of Constraint on Elastic-Plastic Fracture. Steel Research 59, No. 8, 1988, S. 358-367

(6) Clausmeyer, H., Kussmaul, K. and Roos, E. "Influence of Stress State on the Failure Behaviour of Cracked Components Made of Steel". Appl. Mech. Rev. Vol. 44, No 2, (1991), pp. 77-92

(7) Roos, E., Eisele, U., Silcher, H. and Späth, F. "On the Influence of the Material Toughness and the State of Stress on Fracture of Large Scale Specimen". 12. MPA-Seminar, Oktober 1986, Stuttgart

(8) Roos, E., Silcher, H. and Eisele, U. "On 'Lower Crack Resistance Curves' as a Material Law for the Safety Assessment of Components". 15. MPA-Seminar, Oktober 1989, Stuttgart

(9) Katzenmeier, G., Müller-Dietsche, W. "HDR-Sicherheitsprogramm, Gesamtprogramm Phase III". PHDR-Bericht Nr. 0542/88, Kernforschungszentrum Karlsruhe, Oktober 1988

(10) Eisele, U., Restemeyer, D. "Werkstoffuntersuchungen zu den Rohrversuchen E21 und E31". MPA-Prüfungsbericht Nr. 875 021 040 vom 15. April 1991

(11) Schuler, X., Blind, D., Eisele, U. and Herter, K.-H. "Extension of Fracture Mechanics Evaluation Methods by Consideration of Multiaxiality of Stress State for Piping Components". SMiRT 12, August 1993, Stuttgart

(12) Eisele, U., Herter, K.-H., Schuler, X. "Influence of the Multiaxiality of Stress State on the Ductile Fracture Behaviour of Degraded Piping Components". ECF 10, Poster Contribution 63, September 1994, Berlin

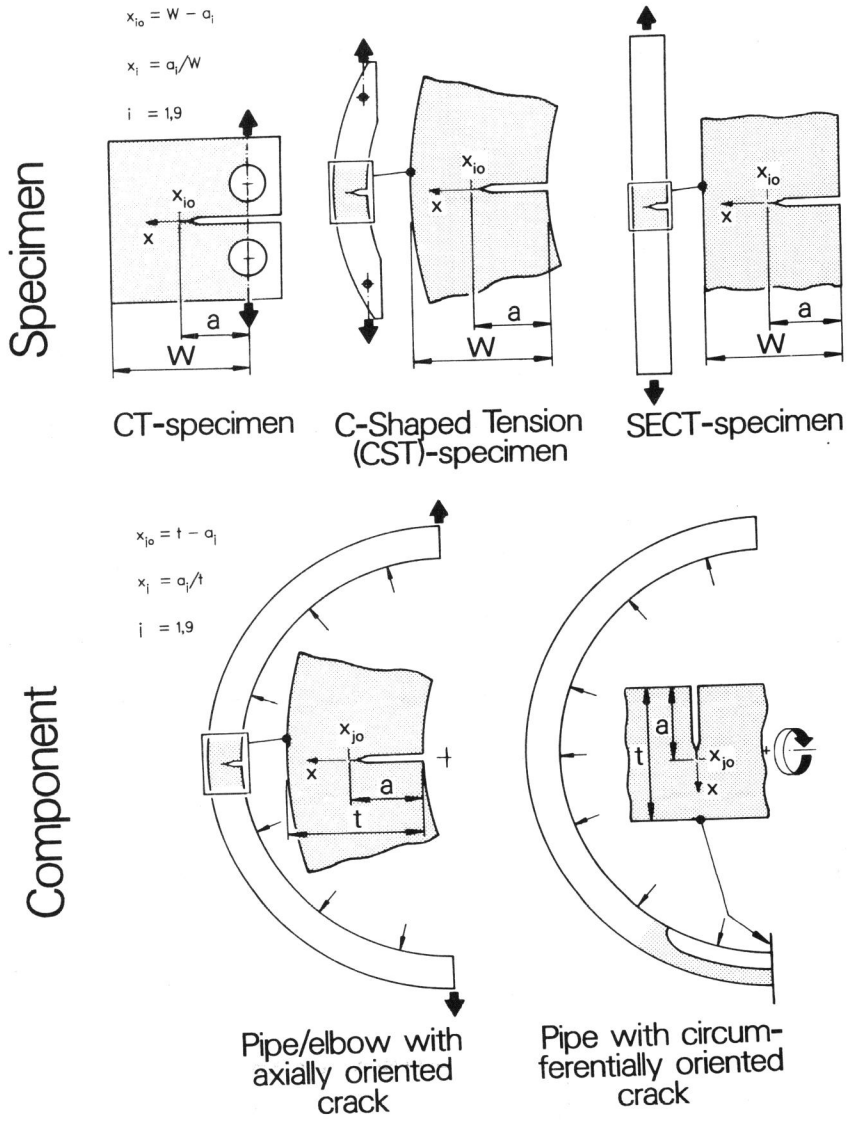

Figure 1 Selected specimen and component geometries

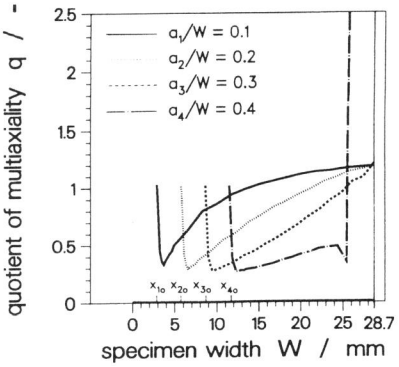

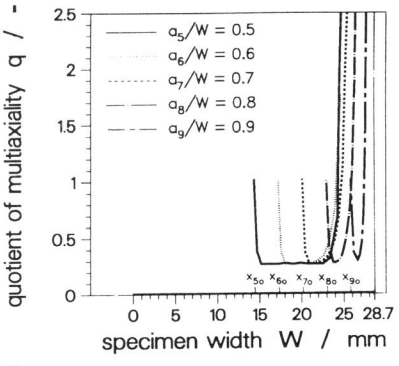

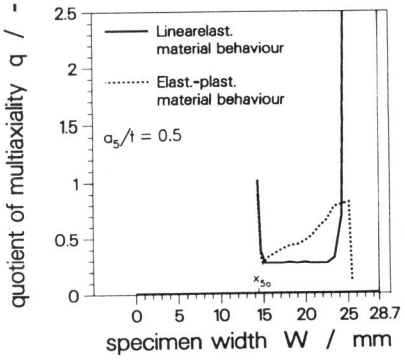

Figure 4 Multiaxiality for SECT-specimen

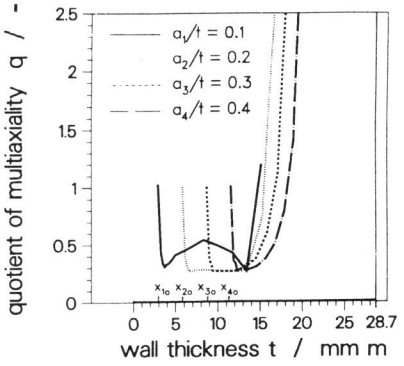

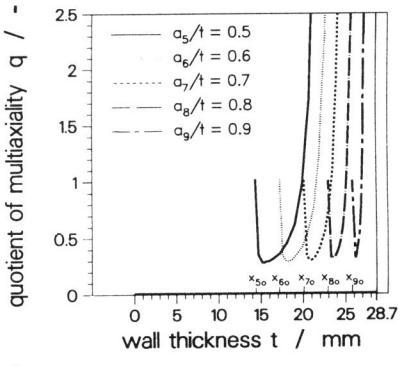

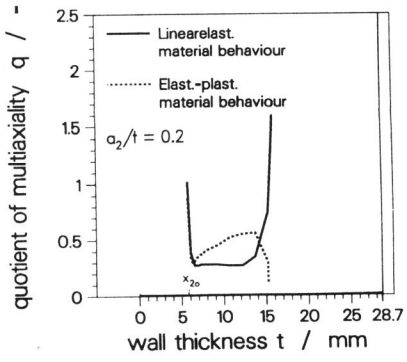

Figure 5 Multiaxiality for axial cracks in elbows under bending

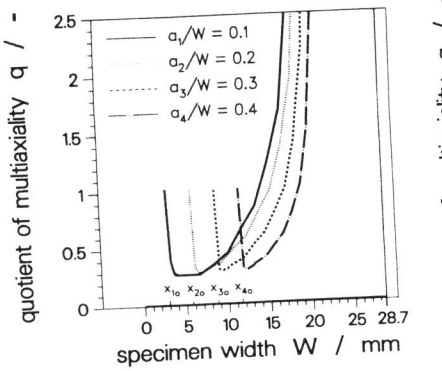

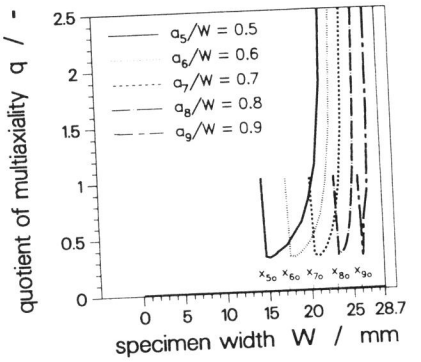

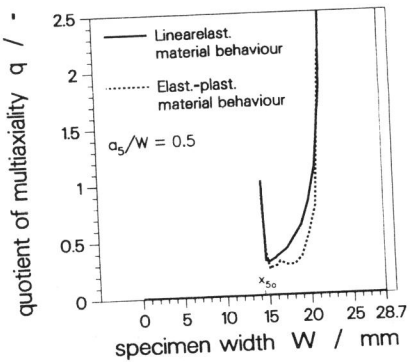

Figure 2 Multiaxiality for CT-specimen

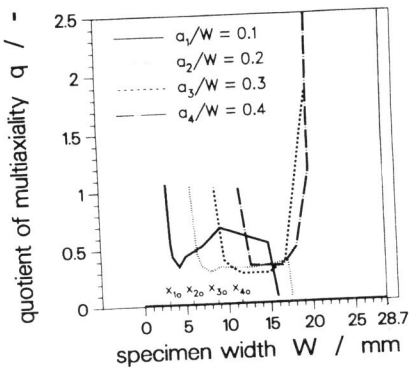

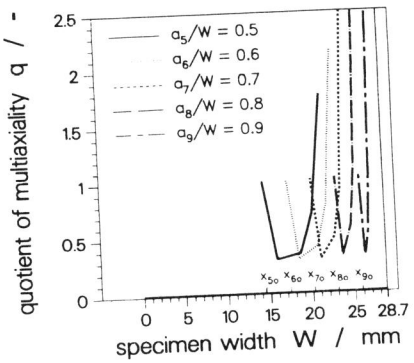

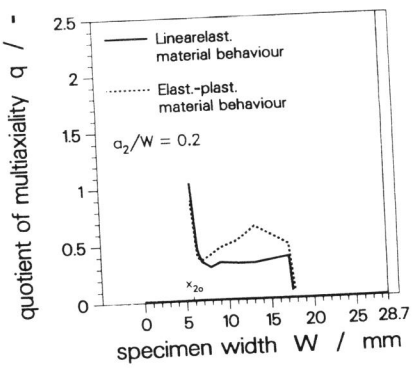

Figure 3 Multiaxiality for CST-specimen

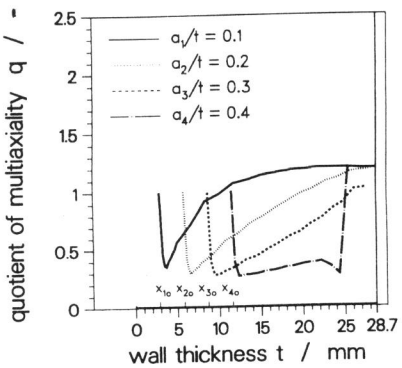

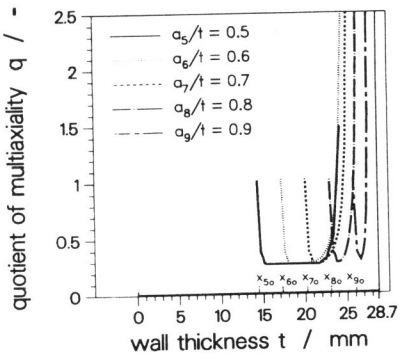

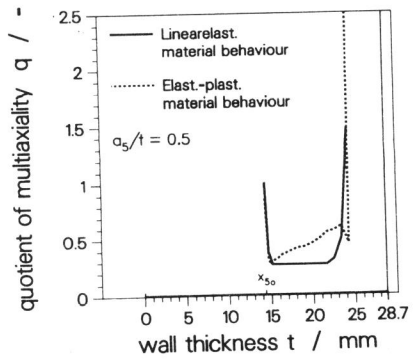

Figure 6 Multiaxiality for axial cracks in pipes/elbows under internal pressure

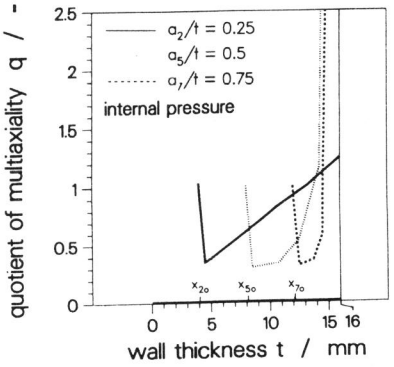

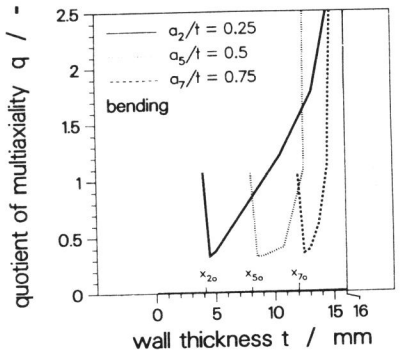

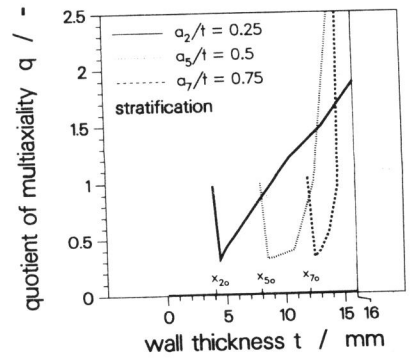

Figure 7 Multiaxiality for circumferential cracks in pipes under internal pressure, bending and stratification

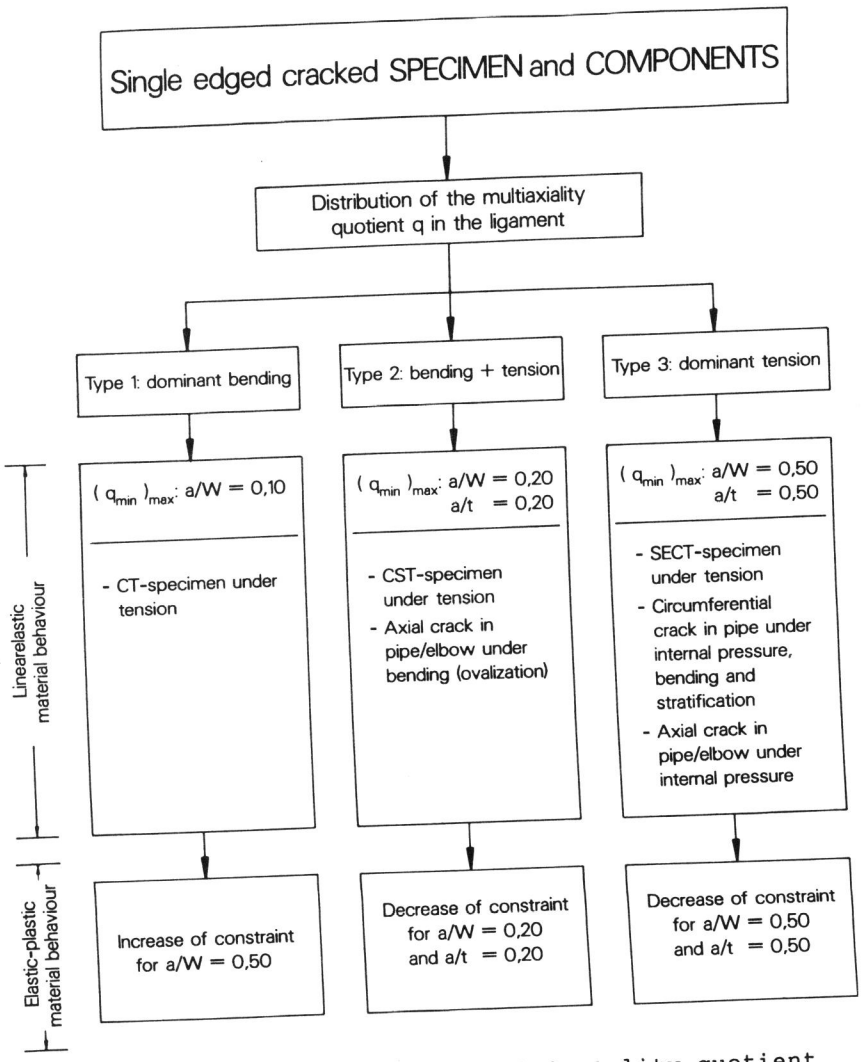

Figure 8 Classification of the multiaxiality quotient distributions